Type IIn supernovae as sources of high energy astrophysical neutrinos

V.N.Zirakashvili, V.S.Ptuskin

Pushkov Institute of Terrestrial Magnetism, Ionosphere and Radiowave Propagation, 142190, Troitsk, Moscow, Russia

arXiv:1510.08387v1 [astro-ph.HE] 28 Oct 2015

Abstract

It is shown that high-energy astrophysical neutrinos observed in the IceCube experiment can be produced by protons accelerated in extragalactic Type IIn supernova remnants by shocks propagating in the dense circumstellar medium. The nonlinear diffusive shock acceleration model is used for description of particle acceleration. We calculate the neutrino spectrum produced by an individual Type IIn supernova and the spectrum of neutrino background produced by IIn supernovae in the expanding Universe. We also found that the arrival direction of one Icecube neutrino candidate (track event 47) is at 1.35° from Type IIn supernova 2005bx.

Keywords:
cosmic rays, supernova, neutrino

1. Introduction

The detection of very high energy astrophysical neutrinos in the IceCube experiment [1, 2, 3] opens up a new possibility for investigation of particle acceleration processes in the Universe. The neutrino production in cosmos is possible via the pp and $p\gamma$ interactions and the decay chains $\pi^+ \rightarrow \mu^+\nu_\mu$, $\mu^+ \rightarrow e^+\nu_e\bar{\nu_\mu}$. The observed astrophysical flux emerges from under more steep air show spectrum at about 50 TeV and has a cutoff at 2 PeV. The neutrino typically carries a small part of the primary proton energy, $E_\nu \approx 0.05E_p$, so the protons with energies up to $E_{\max} \sim 10^{17}$ eV are required to explain the observations (this energy is $\sim 10^{17}$ eV/nucleon in the case of neutrino production by nuclei). Assuming an E^{-2} power-law spectrum, the measured differential flux of astrophysical neutrinos is $E^2F(E) = 2.9 \times 10^{-8}\mathrm{GeV}^{-2}\mathrm{s}^{-1}\mathrm{sr}^{-1}$ for the sum of the three evenly distributed neutrino flavors. The sources of observed neutrinos are not yet identified. The detected 54 events are scattered over the sky and do not show any evident correlation with any astronomical objects [3, 4]. It seems that Galactic sources might account only for a minority of events. The detected astrophysical neutrinos could be produced in extragalactic sources of ultra high energy protons and nuclei. The discussion about potential sources of very high energy neutrinos in the light of the last experimental results can be found in [5, 6, 7] where other useful references are given.

Rare extragalactic Type IIn supernova remnants are considered in the present paper as sources of diffuse high energy neutrinos. It is well established that supernova remnants are efficient accelerators of protons, nuclei and electrons. They are the principle sources of Galactic cosmic rays. The diffusive shock acceleration mechanism suggested in [8, 9, 10, 11] can provide the acceleration of protons and nuclei in the most frequent Type IIP, Ia, Ib/c supernova events up to about $10^{15}Z$ eV that allows to explain the spectrum and composition of Galactic cosmic rays with a proton-helium knee at 3×10^{15} eV and the maximum energy $\sim 10^{17}$ eV where iron nuclei dominate, see [12]. Two orders of magnitude higher $E_{\max} \sim 10^{17}$ eV/nucleon is needed to explain the IceCube neutrino observations. It can be achieved with the Type IIn supernovae that stand out because of extremely dense wind of their progenitor stars with a mass loss rate 10^{-3} – 10^{-1} $M_\odot$ yr^{-1} [13]. As it will be shown below, the large kinetic energy of explosion and very high gas density in the acceleration region lead to the needed energy of accelerated particles and efficiency of neutrino production in pp interactions.

Diffusive shock acceleration by supernova shocks propagating in dense stellar winds was already considered in [14, 15, 16]. Simple analytical estimates showed that radiowaves, gamma-rays and neutrinos might be observable from the nearest Type IIn supernova remnants if the efficient diffusive shock acceleration takes place in these objects. In the present paper we develop this idea further and investigate whether the flux of neutrinos produced in extragalactic Type IIn supernova remnants can explain the IceCube data. For this purpose we perform numerical modeling of particle acceleration in a supernova remnant produced by Type IIn supernova explosion and calculate neutrino production. Our model of nonlinear diffusive shock acceleration describes the remnant evolution and the production of energetic particles. The detailed description of the model was presented in [17] and the simplified version of the model was used in [12] for the explanation of energy spectrum and composition of Galactic cosmic rays. Similar numerical models of diffusive shock acceleration in supernova remnants were developed and employed in [18, 19, 20].

The paper is organized as follows. In the next Sections 2 and 3 we describe modeling of particle acceleration and calculate the spectrum of neutrinos produced in Type IIn supernova remnants. These results are used in Section 4 for calculation of the diffuse neutrino background in the expanding Universe. The discussion of results and conclusions are given in Sections

5 and 6.

2. Nonlinear diffusive shock acceleration model

Details of our model of nonlinear diffusive shock acceleration can be found in [17]. The model contains coupled spherically symmetric hydrodynamic equations and the transport equations for energetic protons, ions and electrons. The forward and reverse shocks are included in the consideration.

The hydrodynamical equations for the gas density $\rho(r,t)$, gas velocity $u(r,t)$, gas pressure $P_g(r,t)$, and the equation for isotropic part of the cosmic ray proton momentum distribution $N(r,t,p)$ in the spherically symmetrical case are given by

$$\frac{\partial \rho}{\partial t} = -\frac{1}{r^2}\frac{\partial}{\partial r} r^2 u \rho \tag{1}$$

$$\frac{\partial u}{\partial t} = -u\frac{\partial u}{\partial r} - \frac{1}{\rho}\left(\frac{\partial P_g}{\partial r} + \frac{\partial P_c}{\partial r}\right) \tag{2}$$

$$\frac{\partial P_g}{\partial t} + u\frac{\partial P_g}{\partial r} + \frac{\gamma_g P_g}{r^2}\frac{\partial r^2 u}{\partial r} =$$

$$-(\gamma_g - 1)\left(\Lambda(T)n^2 + (w-u)\frac{\partial P_c}{\partial r}\right) \tag{3}$$

$$\frac{\partial N}{\partial t} = \frac{1}{r^2}\frac{\partial}{\partial r} r^2 D(p,r,t)\frac{\partial N}{\partial r} - w\frac{\partial N}{\partial r} + \frac{\partial N}{\partial p}\frac{p}{3r^2}\frac{\partial r^2 w}{\partial r}$$

$$+\frac{1}{p^2}\frac{\partial}{\partial p} p^3 b(p) N + \frac{\eta_f \delta(p-p_f)}{4\pi p_f^2 m}\times$$

$$\rho(R_f+0,t)(\dot{R}_f - u(R_f+0,t))\delta(r-R_f(t))$$

$$+\frac{\eta_b \delta(p-p_b)}{4\pi p_b^2 m}\rho(R_b-0,t)(u(R_b-0,t)-\dot{R}_b)\delta(r-R_b(t)) \tag{4}$$

Here $P_c = 4\pi\int dp p^3 v N/3$ is the cosmic ray pressure, $w(r,t)$ is the advection velocity of cosmic rays, T, γ_g and n are the gas temperature, adiabatic index and number density respectively, $D(r,t,p)$ is the cosmic ray diffusion coefficient. The radiative cooling of gas is described by the cooling function $\Lambda(T)$. The function $b(p)$ describes the energy losses of particles. In particular the energy losses due to pp interactions and the radiative cooling are important at early evolutionary stages of IIn supernovae.

Cosmic ray diffusion is determined by particle scattering on magnetic inhomogeneities. The cosmic ray streaming instability increases the level of MHD turbulence in the shock vicinity [9] and even significantly amplify the absolute value of magnetic field in young supernova remnants [21, 22]. It decreases the diffusion coefficient and increases the maximum energy of accelerated particles. The results of continuing theoretical study of this effect can be found in review papers [23, 24]. In our calculations below, we use the Bohm value of the diffusion coefficient $D_B = pvc/3qB$, where q is the electric charge of particles.

Cosmic ray particles are scattered by moving waves and it is why the cosmic ray advection velocity w may differ from the gas velocity u by the value of the radial component of the Alfvén velocity $V_{Ar} = V_A/\sqrt{3}$ calculated in the isotropic random magnetic field: $w = u + \xi_A V_{Ar}$. The factor ξ_A describes the possible deviation of the cosmic ray drift velocity from the gas velocity. We use values $\xi_A = 1$ and $\xi_A = -1$ upstream of the forward and reverse shocks respectively, where Alfvén waves are generated by the cosmic ray streaming instability and propagate in the corresponding directions. The damping of these waves heats the gas upstream of the shocks [25] that is described by the last term in Eq. (3). The heating limits the total compression ratios of cosmic ray modified shocks. In the downstream region of the forward and reverse shock at $R_b < r < R_f$ we put $\xi_A = 0$ and therefore $w = u$.

The magnetic field amplified by cosmic ray streaming instability upstream of the shock is enhanced further via compression in the shock transition region. It can play a dynamical role downstream of the shock. We take magnetic pressure and magnetic energy flux into account downstream of the shock. This is a new element in comparison with our work [17] where the magnetic field spatial distribution was prescribed. The magnetic field is transported in the downstream region as the gas with adiabatic index γ_m. Its impact on the shock dynamics is taken into account via the Hugoniot conditions. Upstream of the forward shock where dynamical effects of magnetic fields are small, the coordinate dependence of the magnetic field B can be described as:

$$B(r) = \sqrt{4\pi\rho_0}\frac{V_f}{M_A}\left(\frac{\rho(r)}{\rho_0}\right)^{\gamma_m/2}, \tag{5}$$

Here ρ_0 and $\rho(r)$ are the undisturbed gas density at the shock position and the density of the medium where the shock propagates respectively, V_f is the speed of the forward shock. The parameter M_A is similar to the Alfvén Mach number of the shock and determines the value of the amplified magnetic field strength far upstream of the shock. In the shock transition region the magnetic field strength is increased by a factor of $\sigma^{\gamma_m/2}$, where σ is the shock compression ratio. The expression similar to Eq.(5) is also used in the upstream region of the reverse shock.

Below we use the adiabatic index of isotropic random magnetic field $\gamma_m = 4/3$. For this value of the adiabatic index, the magnetic pressure $P_m = B^2/24\pi$ is three times smaller than the magnetic energy density ($= B^2/8\pi$).

Two last terms in Eq. (4) correspond to the injection of thermal protons with momenta $p = p_f$, $p = p_b$ and mass m at the forward and reverse shocks located at $r = R_f(t)$ and $r = R_b(t)$ respectively[1]. The dimensionless parameters η_f and η_b determine the efficiency of injection.

We neglect the pressure of energetic electrons and treat them as test particles. The evolution of the electron distribution is described by equation analogous to Eq. (4) with function $b(p)$

[1] We use indexes f and b for quantities corresponding to the forward and reverse (backward) shock respectively.

describing synchrotron and inverse Compton (IC) losses and additional terms describing the production of secondary leptons by energetic protons and nuclei. The secondary electrons and positrons are effectively produced in the dense medium of Type IIn supernova remnant via *pp* interactions. That is why we do not take into account injection of thermal electrons at the shocks in the present calculations.

3. Modeling of diffusive shock acceleration in the remnant of Type IIn supernova

The blast wave produced by Type IIn supernova explosion propagates through the wind of the presupernova star. We assume that the initial stellar wind density profile is described by the following expression:

$$\rho = \frac{\dot{M}}{4\pi u_w r^2}. \quad (6)$$

Here $\dot{M}$ is the mass-loss rate of the supernova progenitor star, u_w is the wind velocity and r is the distance from the center of explosion.

We use the following parameters of the supernova explosion. The explosion energy $E_{SN} = 10^{52}$ erg, ejecta mass $M_{ej} = 10\ M_\odot$, $\dot{M} = 10^{-2}\ M_\odot$ yr^{-1}, the parameter of ejecta velocity distribution $k = 9$ (this parameter describes the power-law density profile $\rho_s \propto r^{-k}$ of the outer part of the ejecta that freely expands after supernova explosion), the stellar wind velocity $u_w = 100$ km s^{-1} that are the characteristic values for Type IIn supernova [13].

The injection efficiency is taken to be independent of time $\eta_b = \eta_f = 0.01$, and the particle injection momenta are $p_f = 2m(\dot{R}_f - u(R_f + 0, t))$, $p_b = 2m(u(R_b - 0, t) - \dot{R}_b)$. Protons of mass m are injected at the forward and reverse shocks. The high injection efficiency results in the significant shock modification already at early stage of the supernova remnant expansion.

Figures (1)-(5) illustrate the results of our numerical calculations. The value of the parameter $M_A = 10$ was assumed.

The dependencies on time of the shock radii R_f and R_b, the forward and reverse shock velocities $V_f = \dot{R}_f$ and $V_b = \dot{R}_b$, cosmic ray energy E_{cr}/E_{SN} are shown in Fig.1.

Radial dependencies of physical quantities at at $t = 30$ yr are shown in Fig.2. The contact discontinuity between the ejecta and the interstellar gas is at $r = R_c = 0.17$ pc. The reverse shock in the ejecta is located at $r = R_b = 0.16$ pc.

We stop our calculations at $t = 30$ yr when the stellar wind mass swept up by the forward shock is of the order of 20 $M_\odot$. This value of the total mass loss is expected if the initial mass of the Type IIn supernova progenitor is $70M_\odot$. The rest goes into ejecta ($\sim 10M_\odot$) and the black hole ($\sim 40M_\odot$). At later times the forward shock enters rarefied medium created by the fast tenuous wind of supernova progenitor at the main sequence stage. So the production of neutrinos becomes negligible at this time.

Spectra of accelerated protons and electrons at $t = 30$ yr are shown in Fig.3. At this point the maximum energy of accelerated protons is about 30 PeV, while higher energy particles

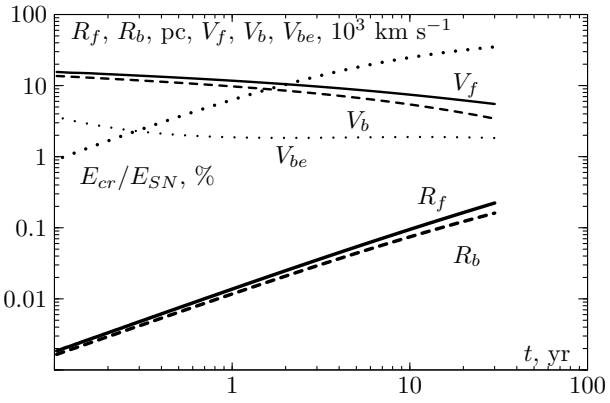

Figure 1: Dependencies on time of the forward shock radius R_f (thick solid line), the reverse shock radius R_b (thick dashed line), the forward shock velocity V_f (thin solid line), the reverse shock velocity V_b (thin dashed line) and the reverse shock velocity in the ejecta frame V_{be} (thin dotted line). The ratio of cosmic ray energy and energy of supernova explosion E_{cr}/E_{SN} (dotted line) is also shown.

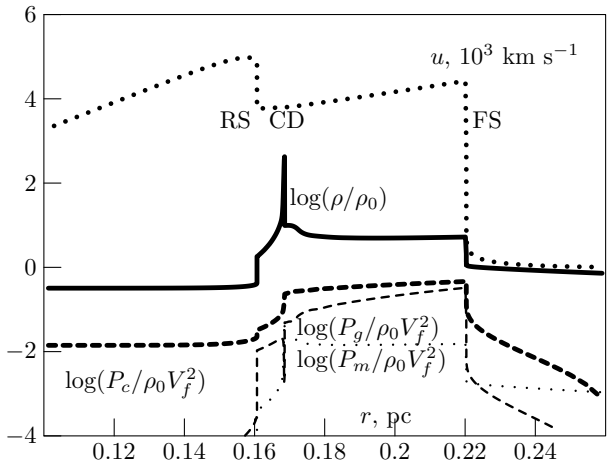

Figure 2: Radial dependencies of the gas density (thick solid line), the gas velocity (dotted line), cosmic ray pressure (thick dashed line) the magnetic pressure (dotted line) and the gas pressure (dashed line) at $t = 30$ yr. At this point the forward shock velocity is $5.5 \cdot 10^3$ km s^{-1}, its radius is 0.22 pc, the magnetic field strength downstream of the forward shock is 0.06 G, the stellar wind density at the current forward shock position $\rho_0 = 10^{-20}$ g cm^{-3}.

have already left the remnant. The maximum energy of protons accelerated at the reverse shock is close to 1 PeV. However, the proton spectrum at the reverse shock goes to higher energies because of the protons coming from the forward shock.

The spectra of particles produced during the life-time of the remnant are shown in Fig.4. They are calculated as the sum of the spectra integrated throughout simulation domain and of the time-integrated outward diffusive flux at the simulation boundary at $r = 2R_f$. About 25% of the kinetic energy of explosion is transferred to cosmic rays.

The temporal evolution of non-thermal emission produced in the supernova remnant at distance 1 Mpc is shown in Fig.5. We take into account a synchrotron self-absorption and a free-free thermal absorption that are important for radio-supernovae [27]. We use the temperature $T = 10^4$K of circumstellar wind that is a characteristic value for dense stellar winds ionized by

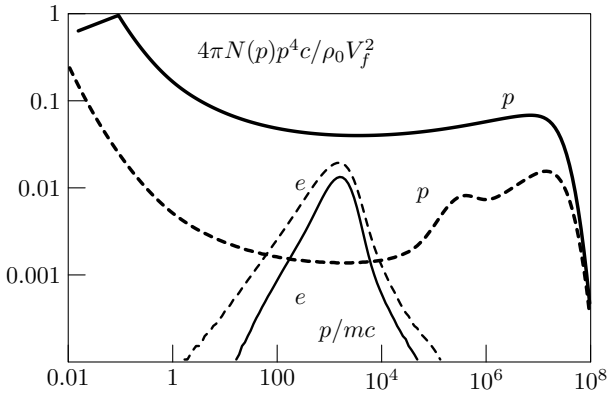

Figure 3: Spectra of accelerated particles at t = 30 yr. The spectrum of protons (thick solid line) and secondary electrons (multiplied on 10^5, thin solid line) at the forward shock, spectrum of protons (thick dashed line) and spectrum of secondary electrons (multiplied on 10^5, thin dashed line) at the reverse shock are shown.

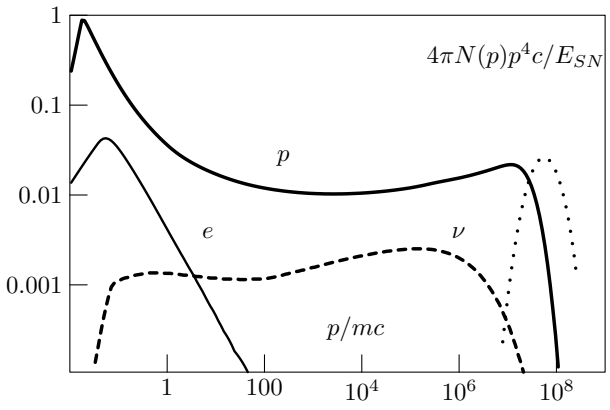

Figure 4: Spectra of particles produced in the supernova remnant during 30 yr after explosion. The spectrum of protons (thick solid line), the spectrum of secondary electrons (multiplied on 10^3, thin solid line), the spectrum of neutrinos (thick dashed line) are shown.

radiation coming from the forward and reverse shocks [28].

It is instructive to compare the results of the present calculations with the approximate analytical expression for the maximum energy of protons accelerated by a supernova shock in the stellar wind. Comparing the acceleration time $10D_B/V_f^2$ with the remnant age t and with the time of pp losses we found the following expression for the maximum energy $E_{\max}$

$$E_{\max} = \frac{3qV_f^2}{10M_A c}\sqrt{\frac{\dot{M}}{u_w}}\min\left(1,\frac{t}{t_{pp}}\right) =$$

$$80\ \text{PeV}\min\left(1,\frac{t}{t_{pp}}\right)\left(\frac{M_A}{10}\right)^{-1}\left(\frac{\dot{M}}{10^{-2}\ M_\odot\ \text{yr}^{-1}}\right)^{1/2}\times$$

$$\left(\frac{u_w}{100\ \text{km s}^{-1}}\right)^{-1/2}\left(\frac{E_{SN}}{10^{52}\ \text{erg}}\right)\left(\frac{M_{ej}}{10\ M_\odot}\right)^{-1} \quad (7)$$

where the time t_{pp} is given by

$$t_{pp} = \frac{0.5c\sigma_{pp}\dot{M}}{\pi u_w m V_f^2} = 0.2\ \text{yr}\left(\frac{\dot{M}}{10^{-2}\ M_\odot\ \text{yr}^{-1}}\right)\times$$

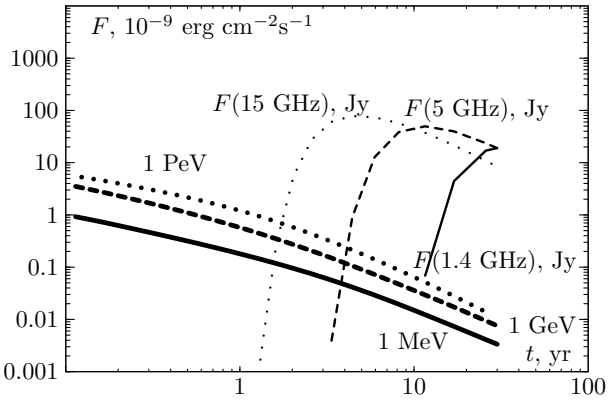

Figure 5: Dependencies on time of fluxes from the supernova remnant at distance 1 Mpc. We show the neutrino flux at 1 PeV produced via pion decay (thick dotted line), the gamma-ray flux at 1 GeV produced via pion decay (thick dashed line). The evolution of the synchrotron gamma-ray flux at 1 MeV (thick solid line) and radio-fluxes at 1.4 GHz, 5 GHz and 15 GHz (thin solid, dashed and dotted lines respectively) are also shown.

$$\left(\frac{u_w}{100\ \text{km s}^{-1}}\right)^{-1}\left(\frac{E_{SN}}{10^{52}\ \text{erg}}\right)^{-1}\left(\frac{M_{ej}}{10\ M_\odot}\right). \quad (8)$$

Here σ_{pp} is the cross-section of pp interactions. For simple estimates we assume that the compression ratio of the forward shock equals to 4 and its velocity $V_f = \sqrt{2E_{SN}/M_{ej}}$ is constant at the free expansion stage.

A similar estimate for Type Ia supernova explosion in the uniform medium gives the "knee" energy $\sim$ 3 PeV for protons. The shocks propagating in stellar winds accelerate particles to higher energies. In particular Type IIn supernova remnants with their dense winds with mass-loss rate $\dot{M} \sim 10^{-2}\ M_\odot\ \text{yr}^{-1}$ can accelerate protons up to 80 PeV according to Eq. (7). This order of magnitude estimate is in agreement with our numerical results illustrated in Fig. 4. Thus, the explanation of proton acceleration up to $\sim 10^{17}$ eV in Type IIn supernova remnants is in line with the acceleration of cosmic rays up to the knee in Type Ia supernova remnants.

4. Calculation of background neutrino flux

Using results of the previous Section, one can calculate the integrated on time number of high-energy neutrinos emitted by a supernova remnant that can be presented by the following equation:

$$Q(E_\nu) = \int dt \int dE \int 4\pi r^2 dr \frac{\rho(r,t)}{m} J_{cr}(E,r,t)\frac{d\sigma(E,E_\nu)}{dE_\nu}. \quad (9)$$

Here we introduced the cosmic ray flux distribution on energy $J_{cr}(E) = 4\pi p^2 N(p)$ and the effective cross section of neutrino production in pp interactions $\frac{d\sigma(E,E_\nu)}{dE_\nu}$, m is the proton mass. The detailed description of the relevant cross sections and kinematics of the neutrino production can be found in [26]. The result of our calculations is shown in Fig.4.

The neutrino spectrum produced by a single supernova remnant $Q(E_\nu)$ can be used for the determination of extragalactic

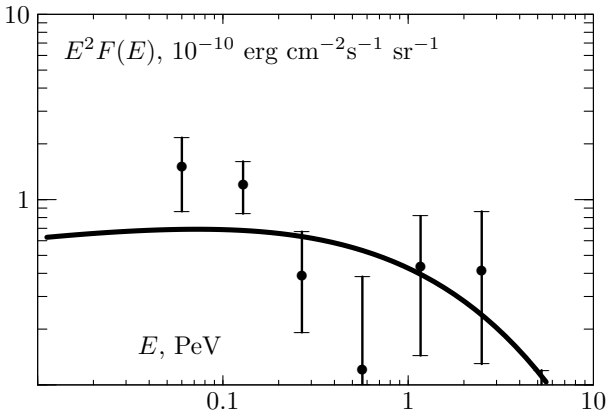

Figure 6: Calculated spectra of neutrino produced by IIn SNRs in the expanding Universe (solid line). IceCube 4 year data [3] are also shown.

neutrino background. Distributed in the Universe Type IIn supernova remnants give the following diffuse flux of neutrinos:

$$F(E_\nu) = \frac{c}{4\pi H_0}\int_0^{z_{\max}} dz \frac{Q((1+z)E_\nu)\nu_{sn}(1+z)^m}{\sqrt{\Omega_m(1+z)^3+\Omega_\Lambda}}$$

$$= \frac{c}{4\pi H_0}\int_{E_\nu}^{(1+z_{\max})E_\nu} dE' \frac{E'^m}{E_\nu^{m+1}} \frac{\nu_{sn}Q(E')}{\sqrt{\Omega_m E'^3/E_\nu^3+\Omega_\Lambda}}. \quad (10)$$

Here the adiabatic energy loss of neutrinos produced at the redshifts $0 \le z \le z_{\max}$ is taken into account. The present neutrino production rate per unit energy and volume is $\nu_{sn}Q(E_\nu)$, where ν_{sn} is the rate of Type IIn supernovae at $z = 0$ while the cosmological evolution of the sources in the comoving volume is described as $(1+z)^m$ ($m = 0$ implies no evolution). The evolution parameter $m = 3.3$ for $z < 1$ and no evolution at $z > 1$, the maximum redshift $z_{\max} = 5$ and the rate $\nu_{sn} = 10^{-6}$ Mpc^{-3} yr^{-1} at $z = 0$ are assumed in our calculations (see e.g. [29]). This rate of Type IIn supernovae is 100 times lower than the rate of all core collapse supernovae. $H_0 = 70$ km s^{-1} Mpc^{-1} is the Hubble parameter at the present epoch, the matter density in the flat Universe is $\Omega_m = 0.28$, and the Λ -term is $\Omega_\Lambda = 0.72$.

The calculated background neutrino spectrum is shown in Fig.6. The figure demonstrates a good fit of our calculations to the IceCube data. We expect that the gamma-ray and neutrino background at energies below 100 TeV are produced by cosmic ray protons via pp interactions in the interstellar medium of galaxies. This explains why the first and the second IceCube data points are above our theoretical curve. In addition the input of atmospheric neutrinos can be significant at these energies.

Using the same approach we can calculate the flux of extragalactic protons. Our results are compared with cosmic ray data in Fig.7. The proton flux produced by extragalactic IIn supernova is below the measured all particle cosmic ray flux and comparable to the measured proton flux at energies $2 \cdot 10^{16}$ eV to 10^{17} eV. The calculated flux is not corrected for possible magnetic horizon effect that can considerably suppress the flux below about 10^{18} eV [30]. The suppression is due to strong deflection of cosmic ray trajectories in extragalactic magnetic fields around the sources in the expanding Universe.

With efficiency of cosmic ray production obtained in our calculations, Galactic Type IIn supernovae could make a significant contribution to the observed intensity of ultra high energy cosmic rays. However the intermittency of infrequent IIn supernova explosions (one in 5 thousand years in the Galaxy) makes the corresponding estimates rather uncertain.

Simple order of magnitude estimates can be done to clarify how the obtained neutrino flux depends on supernova parameters. The main production of high energy particles and neutrinos occurs up to the beginning of the Sedov stage when the shock radius R_S can be determined from the condition $M_{ej} = 4\pi\int^{R_S} drr^2\rho = \dot{M}R_S/u_w$. The time for the beginning of the Sedov stage $t_S = R_S/V_f$ can be written as

$$t_S = \frac{M_{ej}u_w}{\dot{M}V_f} = 10\ \mathrm{yr}\left(\frac{\dot{M}}{10^{-2}\ M_\odot\ \mathrm{yr}^{-1}}\right)^{-1} \times$$

$$\left(\frac{u_w}{100\ \mathrm{km\ s}^{-1}}\right)\left(\frac{E_{SN}}{10^{52}\ \mathrm{erg}}\right)^{-1/2}\left(\frac{M_{ej}}{10\ M_\odot}\right)^{3/2}. \quad (11)$$

We shall assume that at $t > t_{pp}$ the accelerated protons with the spectrum E^{-2} are uniformly distributed in the supernova shell. The neutrino energy flux expected from a supernova at distance D can be estimated as (see also [15, 16])

$$f(E_\nu)E_\nu^2 = \frac{3\xi_{CR}K_\nu}{8\pi\ln(E_{\max}/mc^2)}\frac{V_f^3\dot{M}}{u_w D^2}\left(1+\frac{t}{t_{pp}}\right)^{-1} =$$

$$10^{-8}\frac{\mathrm{erg}}{\mathrm{cm^2 s}}\left(1+\frac{t}{t_{pp}}\right)^{-1} D_{\mathrm{Mpc}}^{-2}\xi_{CR}\left(\frac{\dot{M}}{10^{-2}\ M_\odot\ \mathrm{yr}^{-1}}\right)\times$$

$$\left(\frac{u_w}{100\ \mathrm{km\ s}^{-1}}\right)^{-1}\left(\frac{E_{SN}}{10^{52}\ \mathrm{erg}}\right)^{3/2}\left(\frac{M_{ej}}{10\ M_\odot}\right)^{-3/2} \quad (12)$$

Here ξ_{CR} is the ratio of cosmic ray pressure to the ram pressure of the shock ρV_f^2, $K_\nu \approx 0.25$ is the fraction of energy that goes into neutrinos in pp interactions and $E_{\max}$ is the maximum energy of accelerated protons given by Eq. (7). The value of ξ_{CR} is $\xi_{CR} \sim 0.5$ in our numerical modeling of the efficient cosmic ray acceleration while a lower value $\xi_{CR} \sim 0.1$ is enough to explain the origin of Galactic CRs in supernova remnants.

At early times $t < t_{pp}$ pp losses dominate and the flux is almost steady. It is interesting that the corresponding luminosity $L_\nu \sim 10^{42}$ erg s^{-1} is comparable with the optical luminosity of Type IIn supernovae. This is not surprising because both quantities are determined by the energetics of the forward shock. The optical luminosity can be estimated from relation (see e.g. [13])

$$L = \epsilon\frac{\dot{M}V_f^3}{2u_w}. \quad (13)$$

Here the factor $\epsilon \sim 0.1 - 0.5$. This expression is often used to estimate the mass loss $\dot{M}$ of Type IIn supernova progenitors.

Comparing with Eq. (12) we can rewrite the neutrino flux at $t < t_{pp}$ as

$$f(E_\nu)E_\nu^2 = \frac{3\xi_{CR}K_\nu L}{4\pi D^2\epsilon\ln(E_{\max}/mc^2)} =$$

$$4 \cdot 10^{-12} \frac{\mathrm{erg}}{\mathrm{cm^2 s}} \frac{\xi_{CR}}{\epsilon} 10^{0.4(13.7-m_V)} \quad (14)$$

Here we express the optical flux via the supernova visual magnitude m_V. The similar expression can be used to estimate unabsorbed fluxes of gamma-rays and synchrotron radiation produced by secondary electrons and positrons. The latter scans from radio band to GeV energies for Type IIn supernovae. The unabsorbed gamma ray flux and the flux of synchrotron radiation are lower by a factor of 1.5 and 6 respectively in comparison with the neutrino flux.

Integrated on time expression (12) can be used for the determination of neutrino background produced by all Type IIn supernovae:

$$F(E_\nu)E_\nu^2 = \frac{3\xi_{CR}K_\nu}{16\pi^2 \ln(E_{\max}/mc^2)} \frac{\nu_{sn} c^2 V_f \sigma_{pp} \dot{M}^2}{H_0 m u_w^2} \times$$

$$\ln\left(1+\frac{t_S}{t_{pp}}\right) = 10^{-11}\xi_{CR}\frac{\mathrm{erg}}{\mathrm{cm^2 s\ sr}} \ln\left(1+\frac{t_S}{t_{pp}}\right) \times$$

$$\left(\frac{\dot{M}}{10^{-2}\ M_\odot\ \mathrm{yr^{-1}}}\right)^2 \left(\frac{u_w}{100\ \mathrm{km\ s^{-1}}}\right)^{-2} \left(\frac{M_{ej}}{10\ M_\odot}\right)^{-1/2} \times$$

$$\left(\frac{E_{SN}}{10^{52}\ \mathrm{erg}}\right)^{1/2} \left(\frac{\nu_{sn}}{10^{-6}\mathrm{Mpc^{-3}yr^{-1}}}\right), \quad (15)$$

For parameters used in our modeling the ratio $t_S/t_{pp} \sim 50$. This is far from a so called calorimeter regime $t_S/t_{pp} < 1$ when a significant part of Type IIn supernova explosion energy is transferred to neutrinos. The background flux is several times higher if the cosmological evolution of supernova rate is taken into account (see Eq. (10)). These estimates are valid at neutrino energies $E_\nu < 0.05 E_{\max}$. They confirm the efficiency of high energy neutrino production in supernova explosion in the very dense wind of a progenitor star, as it takes place in the case of Type IIn supernova.

The rate of Type IIn supernovae $\nu_{sn} = 10^{-6}$ Mpc^{-3} yr^{-1} was adjusted in our calculations to reproduce the IceCube observations. Probably the real Type IIn supernova rate is several times higher. However not all Type IIn supernovae have such high mass loss rates and explosion energies as we assumed.

5. Discussion

Our calculations show that the IceCube data can be explained by the neutrinos from Type IIn supernovae. If so, the arrival direction of every IceCube neutrino coincides with the direction to some Type IIn supernova. However, we observe Type IIn supernovae with the redshifts $z \leq 0.1$ while the background is determined by the supernovae with $z \sim 1$. Therefore we expect that only several percent of observed neutrinos i.e. about one or two IceCube neutrino events are associated with the known Type IIn supernovae. Unfortunately, the arrival directions of majority of IceCube neutrinos are known with a low angular resolution (about 15°). Using ASIAGOSN supernova catalogue [2] we found that several Type IIn supernovae are indeed observed in the direction of some IceCube neutrinos. However this result has a low statistical significance.

Nevertheless we note that the arrival direction of one IceCube PeV neutrino candidate (event 20) is within 5° from SN 1978K. This nearest Type IIn supernova in the galaxy NGC 1313 at distance 4 Mpc is for decades observed in radio, X-rays and optics (e.g. [32]). The mass-loss rate of SN 1978K progenitor is estimated as $\dot{M} = 2 \cdot 10^{-3}\ M_\odot$ yr^{-1} [33] that is 5 times lower than we use in our calculations. Thus the fluxes expected from this supernova are not so high as ones shown in Fig.5. In spite of this it is possible that the PeV neutrino candidate was emitted by SN 1978K.

The arrival direction of another IceCube PeV neutrino candidate (event 35) is within 10° from SN 1996cr. This nearest Type IIn supernova in the Circinus galaxy at the same distance 4 Mpc was also detected in radio, X-rays and optics (e.g. [34]). The Circinus galaxy is a bright source of GeV gamma rays [35]. It is known that the forward shock of SN1996cr entered the dense shell of circumstellar matter. The radio flux of this supernova is only several times lower than the flux shown in Fig.5. That is why this IceCube PeV neutrino candidate could be emitted by SN 1996cr.

We also looked for IceCube neutrinos in the vicinity of recent brightest Type IIn supernova 2010jl (m_V =13.5) and 2011fh (m_V =14.5). There were 3 IceCube neutrinos (events 9, 11, 26) within 25° from 2010jl supernova and 2 IceCube neutrinos (events 16, 49) within 10° from supernova 2011fh. Using the measured IceCube neutrino count rate 1.1 neutrino yr^{-1} sr^{-1} we estimate the expected number of 1.2 neutrino per 1.5 year in the vicinity of supernova 2010jl and 0.44 neutrino per 4 year in the vicinity of supernova 2011fh. So it seems that there is some neutrino flux enhancement in the direction of brightest Type IIn supernovae. In addition the first neutrino (event 16) in the vicinity of supernova 2011fh was detected exactly at the time of the supernova discovery.

14 of 54 IceCube neutrinos left tracks in the detector. The arrival directions of these neutrinos are determined with a good angular resolution (about 1°). We found that an arrival direction of one IceCube neutrino candidate (track event 47) is at 1.35° from IIn supernovae 2005bx. The mass-loss rate of this rather distant ($z \sim 0.03$) supernova was estimated as $\dot{M} = 0.037\ M_\odot$ yr^{-1} while the wind velocity $u_w = 813$ km s^{-1} [36]. So the stellar wind density is only a factor of 2 lower in comparison with one used in our calculations. We estimate the radioflux at 5GHz of the order of 1 mJy using radiofluxes shown in Fig.5 and recalculating for 130 Mpc distance to supernova 2005bx.

The expected number of track events within 1.35° from known two hundred Type IIn supernovae is 0.35. Taking into account only supernovae exploded between 2005 and 2014 we reduce this number down to 0.25. The statistical significance will be higher if during the future IceCube operation the neutrino emitted shortly (say 1 year) after supernova explosion will be detected.

[2] https://heasarc.gsfc.nasa.gov/W3Browse/all/asiagosn.html

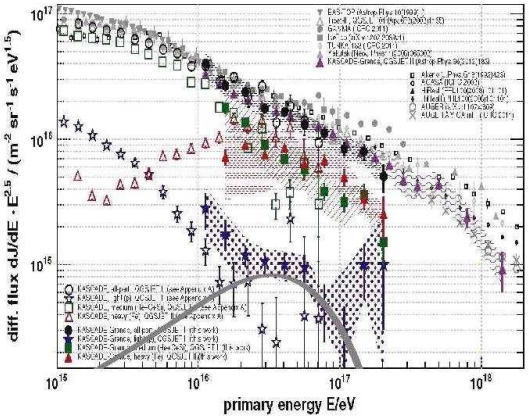

Figure 7: Comparison of the calculated cosmic ray proton background produced by extragalactic Type IIn supernovae (gray solid line) and data on cosmic ray protons and nuclei [31].

Association of the detected by IceCube doublet of neutrino track events with Type IIn supernova was also discussed in [37].

Type IIn supernova were not detected in Gev gamma-rays by Fermi LAT [38]. The upper limit derived corresponds to the ratio $\xi_{CR}/\epsilon \sim 1$ in Eq. (14).

6. Conclusions

Our main conclusions are the following:

1) The diffusive shock acceleration of particles in Type IIn supernova remnants and the production of neutrinos via pp interactions in the dense presupernova winds can explain the diffuse flux of high energy astrophysical neutrinos observed in the IceCube experiment.

2) The calculated maximum energy of protons accelerated in Type IIn supernova remnants is close to 10^{17} eV. This value is higher than the maximum energy achieved in the main part of SNRs and is explained by the high density of the circumstellar matter.

3) The efficient acceleration of particles and production of secondary electrons and positrons result in the fluxes of radiowaves and gamma-rays that can be observed from the nearest Type IIn supernova remnants.

4) Future IceCube operation and the search of correlations between neutrino arrival directions and the directions to Type IIn supernovae may check whether these objects are the sources of high energy neutrinos but only one track event during 10 years is expected from these supernovae with the redshifts less than 0.1. The bright phase of a Type IIn supernova remnant as a source of PeV neutrinos lasts for about several years after the supernova explosion.

The work was supported by the Russian Foundation for Basic Research grant 13-02-00056 and by the Russian Federation Ministry of Science and Education contract 14.518.11.7046.

References

[1] Aartsen, M.G., Ackermann, M., Adams, J. et al. 2013, Science 342, 1242856
[2] Aartsen, M.G., Ackermann, M., Adams, J. et al. 2014, Phys. Rev. Lett., 113, 1101
[3] IceCube Collaboration, 2015, Proc. 37th ICRC, 30 July-6 Aug, Hague, Netherlands, Pos(ICRC2015) 1081
[4] Aartsen, M.G., Ackermann, M., Adams, J. et al. 2014, ApJ, 796, 109
[5] Anchordoqui, L.A., Barger, V., Cholis, E. et al. 2014, JHEAp, 1, 1
[6] Gaisser, T. & Halzen F. 2014, Annu. Rev. Nucl. Part. Sci. 64, 101
[7] Murase, K 2014, arXiv:1410.3680v2
[8] Krymsky, G.F. 1977, Soviet Physics-Doklady, 22, 327
[9] Bell, A.R., 1978, MNRAS, 182, 147
[10] Axford, W.I., Leer, E. & Skadron, G., 1977, Proc. 15th Int. Cosmic Ray Conf., Plovdiv, 90, 937
[11] Blandford, R.D., & Ostriker, J.P. 1978, ApJ, 221, L29
[12] Ptuskin, V.S., Zirakashvili, V.N. & Seo, E.S. 2010, ApJ, 718, 31
[13] Moriya, T.J., Maeda, K., Taddia, F., Sollerman, J., Blinnikov, S.I., & Sorokina, E.I., 2014, MNRAS 439, 2917
[14] Murase, K., Thompson, T.A., Lacki, B.C., & Beacom, J.F., 2011, Phys. Rev. D, 84, 043003
[15] Katz, B., Sapir, N., & Waxman, E., 2011, arXiv.1106.1898
[16] Murase, K., Thompson, T.A., & Ofek, E.O., 2014, MNRAS 440, 2528
[17] Zirakashvili, V.N. & Ptuskin V.S. 2012, Astropart. Phys. 39, 12
[18] Berezhko, E.G., Elshin, V.K. & Ksenofontov, L.T., 1994, Astropart. Phys. 2, 215
[19] Kang, H. & Jones, T.W. 2006, Astropart. Phys. 25, 246
[20] Berezhko, E.G., & Völk, H.J., 2007, ApJ, 661, L175
[21] Bell, A.R., 2004, MNRAS, 353, 550
[22] Zirakashvili, V.N. & Ptuskin, V.S., 2008, ApJ 678, 939
[23] Bell, A.R., 2014, Astropart. Phys. 43, 56
[24] Caprioli, D., 2014, arXiv:1410.1644v1
[25] McKenzie, J.F., & Völk, H.J., 1982, A&A, 116, 191
[26] Kelner, S.R., Aharonian, F.A. & Bugayev, V.V., 2006 Phys. Rev. D74, 034018
[27] Chevalier, R., 1998, ApJ 499, 810
[28] Lundqvist, P., & Fransson, C., 1988, A&A 192, 221
[29] Dahlen, T., Strolger, L.-G., Riess, A.G. et al., 2012, ApJ, 757, 70
[30] Aloisio, R., Berezinsky, V.S., 2005, Astrophys.J., 625,249
[31] Apel, W.D., Arteaga-Velázquez, J.C., Bekk, K. et al. 2013, APh 47, 54
[32] Smith, I.A., Ryder, S.D., Böttcher, M., et al., 2007, ApJ, 669, 1130
[33] Chugai, N.N., Danziger, I.J., & Della Valle, M., 1995, MNRAS, 276, 530
[34] Bauer, F.E., Dwarkadas, V.V., Brandt, W.N. et al., 2008, ApJ, 688, 1210
[35] Hayashida, M., Stawarz, L., Cheung, C.C., et al. 2013, ApJ, 779, 131
[36] Kiewe, M., Gal-Yam, A., Arcavi, I., et al., 2012, ApJ 744, 10
[37] Aartsen, M.G., Abraham, K., Ackermann, M., et al. 2015, Astrophys.J., 811, 52
[38] Ackermann, M., Arcavi, I., Baldini, L. et al. 2015, Astrophys.J., 807, 169